Structural Engineering and Mechanics, Vol. 46, No. 3 (2013) 371-385 371
DOI: http://dx.doi.org/10.12989/sem.2013.46.3.371

The dynamic response of a prototype steel floor using velocity-source type of excitation

Max D.C. Magalhaes*

Department of Structural Engineering, Federal University of Minas Gerais, Belo Horizonte 31270-901, Brazil

(Received September 1, 2012, Revised April 2, 2013, Accepted April 9, 2013)

Abstract. Vibration isolators and anti-vibration mounts are ideal, for example, in creating floating floors for gymnasiums, or performance spaces. However, it is well-known that there are great difficulties on isolating vibration transmission in structural steel components, especially steel floors. Besides, the selection of inertia blocks, which are usually used by engineers as an effective vibration control measure, is usually based on crude methods or the experience of the engineers. Thus, no simple method or indices have been available for assessing the effect of inertia blocks on vibration isolation or stability of vibratory systems. Thus, the aims of this research are to provide further background description using a FE model and present and implement a modal approach, that was validated experimentally, the latter assisting in providing improved understanding of the vibration transmission phenomenon in steel buildings excited by a velocity-source type of excitation. A better visualization of the mean-square velocity distribution in the frequency domain is presented using the concept of modal expansion. Finally, the variation of the mean-square velocity with frequency, whilst varying mass and/or stiffness of the coupled system, is presented.

Keywords: steel floor; FE simulations; dynamic response; velocity excitation

1. Introduction

In general, mechanical and/or civil engineers designs and installs anti-vibration mounts to combat structure-borne noise and vibration. Vibration isolation of building services equipment is an accepted and essential part of every heating, ventilating and air conditioning (HVAC) installation. Nowadays, modern buildings are constructed using lighter structures than in the past. This means they require greater protection if noise and vibration are to be prevented from being structurally transmitted to critical areas. Thus, it is essential to think on ‘anti-vibration’ solutions that effectively combat such structure-borne noise and vibration. There exist an extensive range of vibration isolation equipment including pads, springs and hangers. Vibration isolators and anti-vibration mounts are ideal, for example, in creating floating floors for gymnasiums, or performance spaces.

In building acoustics, a floating floor system is a construction technique where a resilient quilt is laid directly on a concrete floor slab (structural floor) and turned up at the edges against the abutment walls. Subsequently, a floating screed is laid over the resilient quilt. For vibration

*Corresponding author, Associate Professor, E-mail: maxdcm@gmail.com

reduction purposes, our main interest is in the low frequency range. For the evaluation of the effectiveness of vibration reduction measures in the transfer path, it has to be know also what happens with the excitation.

There are many situations where a number of vibrational sources contribute to a total noise problem via a number of different transmission paths. Vibration control technology is concerned primarily with isolating the contribution of each separate source so that appropriate treatment may be applied in a cost-effective manner to those sources which contribute most strongly. Mondot and Petersson (1987) proposed a characterization of structure-borne sound sources in terms of source descriptors by using the free velocity and source mobility at the contact point. More studies (Fulford and Gibbs 1999, Petersson and Gibbs 2000) have been conducted to determine the vibration velocities, transmitted forces, and transmitted power for a resiliently supported machine. However, these studies have been primarily devoted to the characterization of structure-borne sound sources instead of the development of an engineering method for vibration isolation. Mak and Su (2002) recently proposed the power transmissibility method to assess the performance of vibration isolation. Based on the total structure-borne sound power transmission, this method takes into account the dynamic characteristics of structure-borne sound emission and the interaction of mounting points.

Although it is a complex matter, it is useful to consider whether the structure is excited by a force or velocity source. For a force source, the driving point impedance of the source at the interface with the excited structure is low compared to the impedance of this structure. On the other hand, if we assume a velocity source, the impedance of the source is much greater than the impedance of the receiver, i.e. the structure. For many applications one of these extremes is appropriate to evaluate the effect of design changes.

Resilient vibration isolators and inertia blocks are very popular among engineers to reduce structure vibration that is transmitted from a machine, such as a compressor, to the floor structure. Vibration isolators are usually selected in practice according to the force transmissibility method (Rao 1995, Cremer *et al*. 2005). However, this method oversimplifies the vibration power transmission from the machine to the floor structure and does not consider the interaction of mounting points and the dynamic characteristics of the floor. Although there are many similarities among the vibration mechanisms studied by a variety of researches, there are also differences in the approaches used. There is uncertainty about how the vibration approaches developed on the basis of simple vibration mechanisms can be extended or interpreted for cases where a structure vibrates in a more complex way.

Computational techniques such as the Finite Element and Boundary Element Methods are available for treating radiation from structural plates. The formulation of a numerical model that can predict the transmission of impulsive sound from outdoors to indoors at low frequencies was presented by Remillieux (2012). Although the model for the external pressure loading was adapted to building structures with rather general geometries (with the only constraint of having flat surfaces), the vibro-acoustic model was limited to building components with 2-D geometries backed by rectangular cavities. The experimental validation of the model was also presented for two cases of increasing complexity. It was demonstrated that numerical predictions were in good agreement with experimental data. Vigoureux and Guyader (2012) presented one application of a new method, namely Time Reversal method, to structural vibrations of complex industrial systems and describe the parameters that increase or decrease the efficiency of the method. The application of the Time Reversal method in this particular context might be particularly useful when it is not possible to directly measure the vibration field on the structure, which would be the case for testing working machineries.

Another important mechanism related to structure vibration is the radiated sound field which is a problem shared by many researchers in the field of engineering acoustics (Langley 2007, Leppington *et al*. 1982). The mechanism of sound transmission may be considered in terms of the radiated sound field from an elastic partition, itself excited by a dynamic force. The partition, modelled by a thin plate, has a response to force and/or velocity excitation, which consists of both free and forced bending waves. Freely travelling bending waves are generated when the plate is excited at its natural frequencies. As a result of the plate edges, these waves interact with each other producing the plate mode of vibration. On the other hand, forced waves occur due to pressure fluctuations which force the plate to move in such a way that free-bending waves are not significantly generated. The spatial distribution of the forcing produces a response that is similar in its spatial response.

In terms of radiation efficiency, which is a non-dimensional measure of the sound power radiated by a vibrating surface into an adjacent fluid, the generation of free bending waves is more important at frequencies above the critical frequency of the panel, where the natural modes of the partition consist of wave motion with phase velocity greater than the speed of sound travelling in air. In this condition, sound power is radiated efficiently. Below the critical frequency, the free waves are produced but are not significant for sound transmission. Forced waves at the acoustic wave number are predominant when a panel vibrates at frequencies lower than its critical frequency. They are common when a panel is excited acoustically. In addition, when a sound wave is incident upon a partition, the response, which is frequency dependent, is also dependent on the radiation impedance of the modes of the partition. Thus, the air or fluid on the receiver side of the plate is excited, and sound waves propagate away from the plate into the receiving volume. Below the first panel resonance, there is an increase in the Sound Reduction Index (SRI) with decreasing frequency. In this frequency range, the panel moves with the pressure fluctuation to transmit sound and has a very small frequency response. The vibration can be reduced by stiffening the panel hence causing an increase in the SRI (Fahy 1985).

This paper is aimed at providing not only a better understanding of the vibration transmission mechanism in itself but also to produce a useful set of data which for instance can be used by vibration control engineers as, for example, input data for a Statistical Energy Analysis. This data might be useful for optimizing vibration isolation in buildings at low frequencies, where the modal behaviour of floors strongly influences the transmission. Some results are compared to those obtained using classical boundary conditions, such as the simply-supported, clamped and free boundary cases. Conclusions on the use of this alternative method and its subsequent application to structural radiation problems are briefly presented.

2. Methodology

In this section, the methodology used for the vibration transmission investigation is presented. First, a Finite Element (FE) model is developed in order to simulate the dynamic characteristics of two distinct systems: one represented by a steel plate and another one which consists of a floating system. Using the FE model, the natural frequencies (and their corresponding vibration modes) and Frequency Response Function (FRF), named mobility, were obtained. Second, experimental tests are made in order to validate the numerical model. They consisted of preliminary studies and FRF data acquisition and analysis. Third, a parametric study is performed. It was based on the development of a modal model to analyze the influence of the floating mass and isolator stiffness on the variation of vibration levels with frequency range. As mentioned previously, in this paper it is assumed that the impedance of the source, which is represented by a compact mass subjected to an impulse force, is much greater than the impedance of the receiver. In other words, a velocity source model was considered on all simulations and experimental tests.

2.1 The finite element models

Numerical simulations are presented for a prototype of a real steel floor. The prototype consists of a scaled four-point simply-supported steel plate commonly used on the process of building design. FE models were considered in order to find the corresponding normal modes for this specific boundary conditions. The first one based on a four-point simply-supported plate (see Fig. 1) and the second one consists of the same plate attached to a block mass (e.g., representing the screed) with a resilient pad under it (see Fig. 2). A frequency range of 10-70 Hz was considered on the analysis. Figs. 1 and 2 show the FE model mesh generated for the four-point simply-supported steel plate. The mesh consisted of 3,753 elements. Thus, it was ensured a minimum of 6 elements per structural wavelength λ_b (= $2\pi/k_b$) at 200 Hz, which was the maximum frequency considered. It is seen the natural frequencies and corresponding mode shapes $\phi_p(z,y)$ obtained for the first five modes.

The analyses were performed on two distinct stages as follow: Firstly, the commercial FE software, namely ABAQUS (2005), was used in order to obtain the mode shapes (and their corresponding natural frequencies) for the four-point simply-supported plate, and consequently to validate the FE model against its analytical counterpart. The plate was modeled using shell elements (see Fig. 1). Secondly, FE simulations were performed for the floating system. Likewise the corresponding sets of normal modes $\phi_p(z,y)$ were extracted and stored. The block mass and the resilient material were both modeled using 3D Solid Elements. In other words, the FE model was composed of a mass-spring-plate model (see Fig. 2). The structural subsystem corresponds to the interaction between a floating screed (M_m = 2.6 kg), a resilient quilt (E_k = 1.5MPa, ζ_k = 0.05) and a flexible structural plate (ρ_p 7,580kg/m^3; E_p = 210 GPa).

The height of the steel block was 50mm. A total loss factor equal to 0.02 was adopted for the steel plate. The floor dimensions considered herein was equal to L_{px} = 700 mm, L_{pz} = 800 mm and h = 5mm. The thin plate theory was appropriate herein. The basis of the criterion for 'thinness' adopted was $k_b h_p < 1$; where k_b is the free structural wavenumber and h_p is the plate thickness. For all simulations, one point load equal to 1 kN was applied at the point F1(z_0, y_0) where x_0 = 540 mm, z_0 = 665 mm.

In Fig. 1 the excitation points are defined by F1(54.0; 66.5),F2(55.5; 32.5), F3(28.5; 30.0), F4(50.0; 48.5). Likewise, the response points are RP1(55.0; 0.0), RP2(35.5; 42.0), RP3(0.0; 65.0), RP4(11.0;10.0). The unit considered is centimeter.

Likewise, in Fig. 2 the excitation (F) and response (RP) point locations are: F1(54.0; 66.5),F2(55.5; 32.5), F3(28.5; 30.0), F4(50.0; 48.5) and RP1(55.0; 0.0), RP2(35.5; 42.0), RP3(0.0; 65.0), RP4(11.0;10.0) respectively. The unit considered is also in centimeter.

2.2 Experimental tests

The structure was a steel plate (700mm × 800 mm × 5mm) simply-supported on four points near to its corners. The plate was directly supported by four bolts (ϕ = 10mm) located 3.5cm from

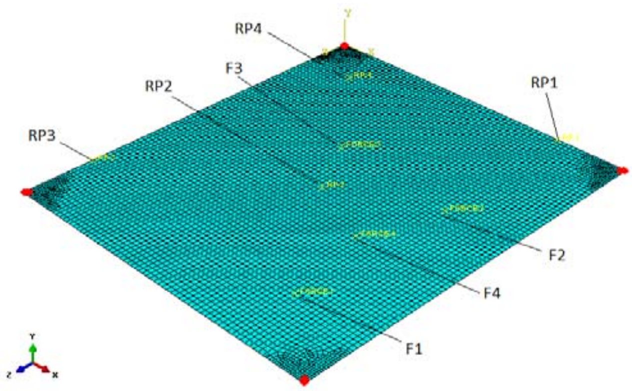

Fig. 1 Impulse excitation (F) and response (RP) locations

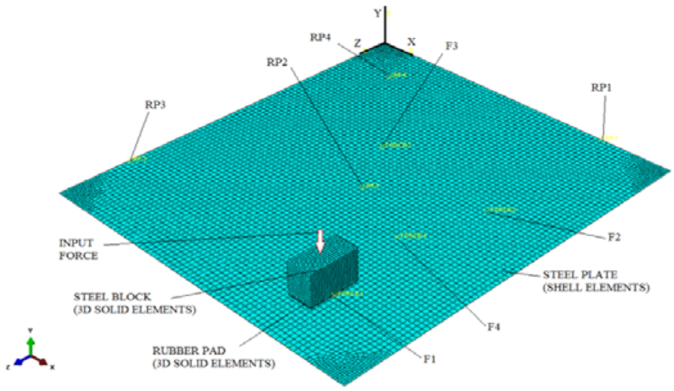

Fig. 2 Impulse excitation (F) and response (RP) locations considering the block mass

the plate edges. The bolts were clamped to a massive concrete floor. The boundary conditions along the plate edges were free. A steel block (50 mm × 65mm × 100mm) representing for instance, a machine to be isolated, was placed on the plate. Measurements were made with the block with and without a pad isolator (see Fig. 3 below). The value estimated for s' was 0.3 GN/m^3 (Sanz *et al*. 2011). The Young's modulus can be estimated by considering that the dynamic stiffness is inversely proportional do the thickness of the specimen

$$E = s'.h \tag{1}$$

where h is the thickness of the specimen.

Therefore, the longitudinal Young's modulus was then equal to E_{rubber} = 1.5 MPa. The damping ratio of the rubber was considered equal to ζ_{rubber} = 0.05 (Sanz *et al*. 2011).

First, the aim was to measure the natural frequencies of the four-point supported steel plate using the frequency response functions (FRFs) defined by Fahy (1985)

$$H_{ji} = \frac{s_{ij}}{s_{ii}} [\text{m.s}^{-2}/\text{N}] \tag{2}$$

where s_{ij} and s_{ii} are the cross-spectral density function (for a force applied at point i and the corresponding velocity measured at point *j*) and the autospectral density function (for a force applied at point *i*) respectively. These functions were obtained via Fourier transforms of the measured quantities. These functions are also named mobilities or velocity transfer functions. The vibration source was a plastic-headed hammer. It was used to hit the steel plate at different locations (in order to obtain the H_{ji}) over a period of 8 seconds. The point mobility of the system was obtained by measuring the impact force and the acceleration, which was later integrated in order to obtain the velocity. The average vibration level of the steel plate was measured for three distinct conditions: first, an impulsive force was applied directly at the steel plate; second, the same force was applied at the steel block placed on the same location on the plate; third, the impulsive force was applied on the 'floating' block supported by the rubber placed over the steel plate (see Fig. 3 below). The velocities were determined by integrating the accelerations at every frequency line.

The FRF 'sweeps' using the instrumented hammer resulted in 16 FRFs which were acquired over four response and four excitation test points as a reference. A simple technique used in Cremer *et al*. (2005) helps the selection of frequencies which may correspond to the modes of vibration. Thus, another simple parameter named Mode Indicator Function (MIF) denoted as

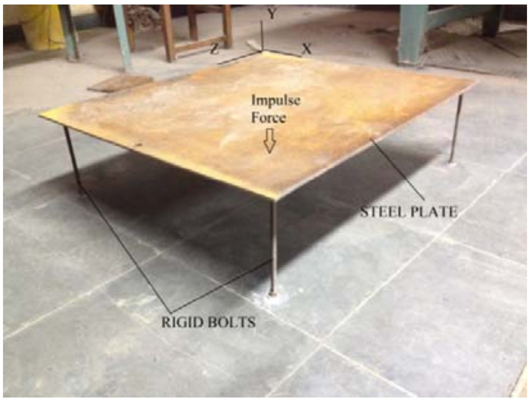

(a) Steel plate supported at 4 points without a block mass between the force and the plate

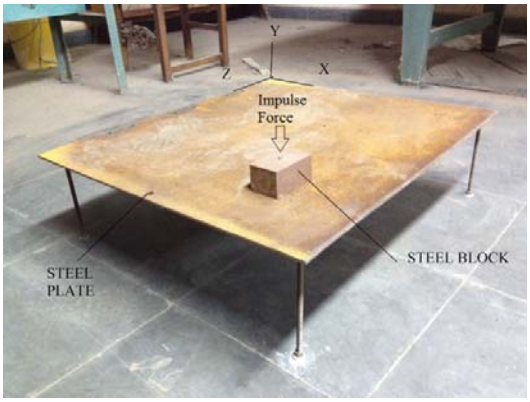

(b) Steel plate supported at 4 points with steel block mass directly supported by the plate

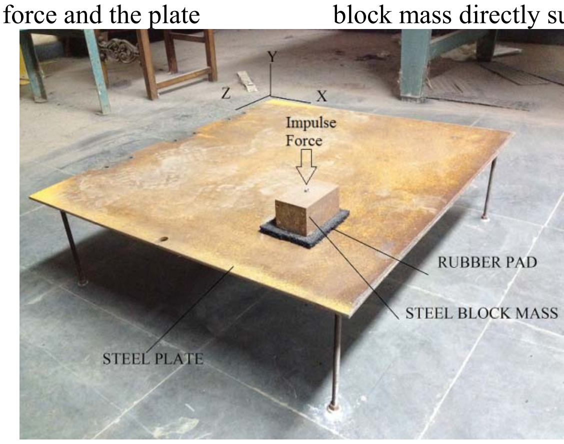

(c) Steel plate supported at 4 points with floating block (block directly supported by a rubber pad

Fig. 3 Measurement setup

$|H_{j,sum}(\omega)|$ and defined as the sum of the moduli of all measured FRFs, was selected. It is given by Pavic and Reynolds (2003)

$$|H_{j,sum}(\omega)| = \sum_i H_{ji}(\omega) \quad (3)$$

In general four methods for comparing analytical and/or FE models to experimental modal properties are most used: comparison of natural frequencies, comparison of mode shapes, modal assurance criterion (MAC) and performance of a particular degree of freedom (Brownjohn and Xia 2000). In this paper, only the comparison of natural frequencies is made.

3. Results and discussion

In this section the results are presented for the numerical, experimental and analytical models.

3.1 Dynamic response of a four-point simply supported plate

In Fig. 4 the first five modes and natural frequencies of the four-point simply supported steel plate are presented. They were obtained via a Finite Element model. It is seen that symmetric and anti-symmetric modes do exist in the frequency range 10Hz-70Hz. Table 1 below presents a comparison between the measured and estimated (FE model) natural frequency values.

It is observed in Table 1, the relationship between measured and calculated natural frequencies. There were significant correlations with values ranging from 94.9% to 99.6%.

Fig. 5 shows the variation of the MIFs with frequency for the steel plate. The calculation was based on the summation of the columns of FRF matrix corresponding to the rows: a) RP1 (j = 1); b) RP2 (j = 2); c) RP3 (j = 3); d) RP4 (j = 4). The peaks in the curves indicate the frequency of the possible modes of vibration. It is seen some similarities as resonance frequencies obtained via the FE model and measured data are compared.

Table 1 Comparison between measured and predicted natural frequencies of the four-point simply-supported plate

Vibration Mode Number	F_N [Hz] (FE model)	F_N [Hz] (Measured)	Correlation %
1	13.2	12.8	99.6
2	27.9	29.3	98.6
3	28.8	32.7	96.1
4	45.3	46.8	98.5
5	60.6	65.7	94.9

As frequency increases, the correlation between numerical and measured peaks decreases. It appears that those discrepancies are closely related to the structural response of the partition which for instance depends on structural coupling and/or damping effects. The deviation of the predicted values from those obtained experimentally may also be due to the poor signal-to-noise ratio values.

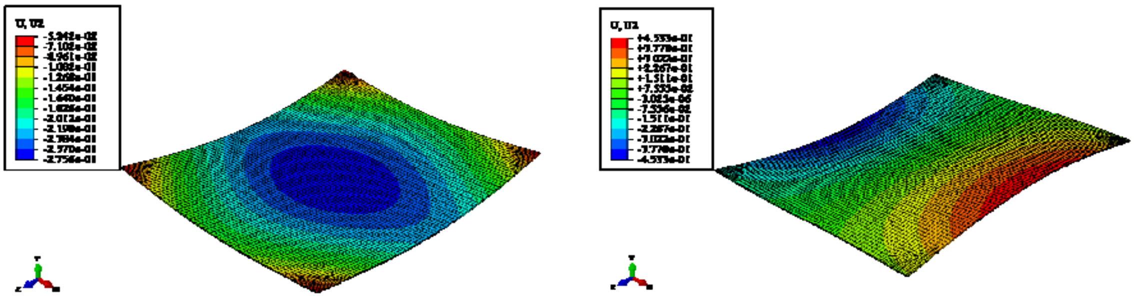

(a) $f_1 = 13.2$ Hz (1st mode) (b) $f_2 = 27.9$ Hz (2nd mode)

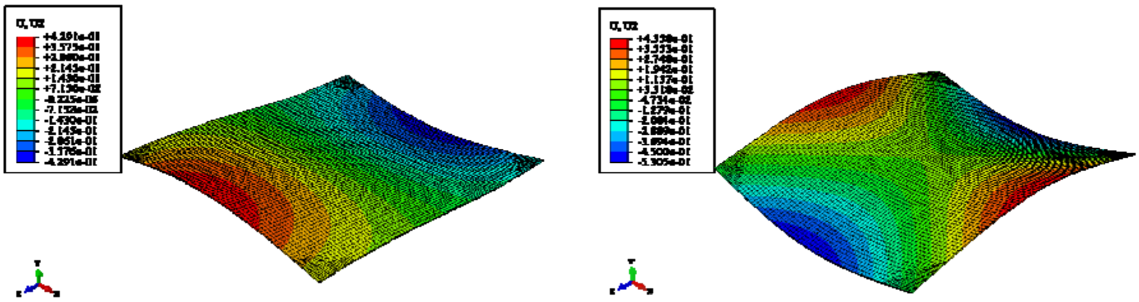

(c) $f_3 = 28.8$ Hz (3rd mode) (d) $f_4 = 45.3$ Hz (4th mode)

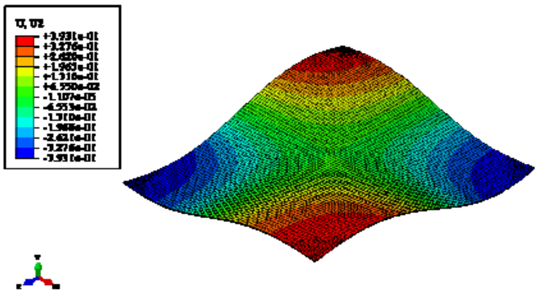

(e) $f_5 = 60.6$ Hz (5th mode)

Fig. 4 Modes and natural frequencies of the steel plate

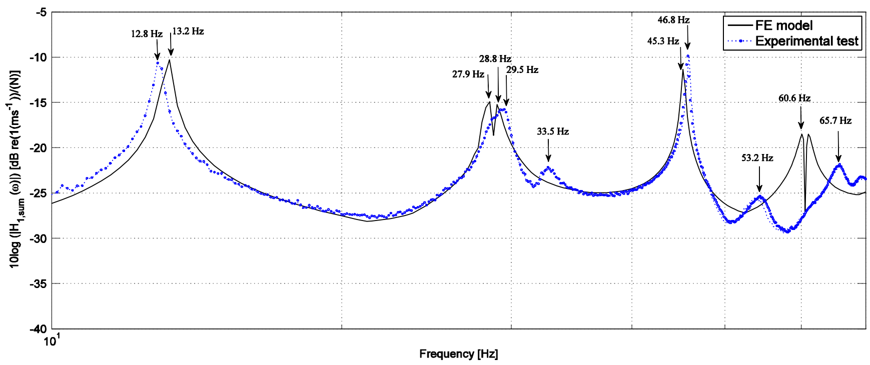

(a) RP1 ($j = 1$)

Fig. 5 Variation of the MIFs with frequency for the steel plate. The calculation was based on the summation of the row FRF matrix corresponding to the reference response points RPs

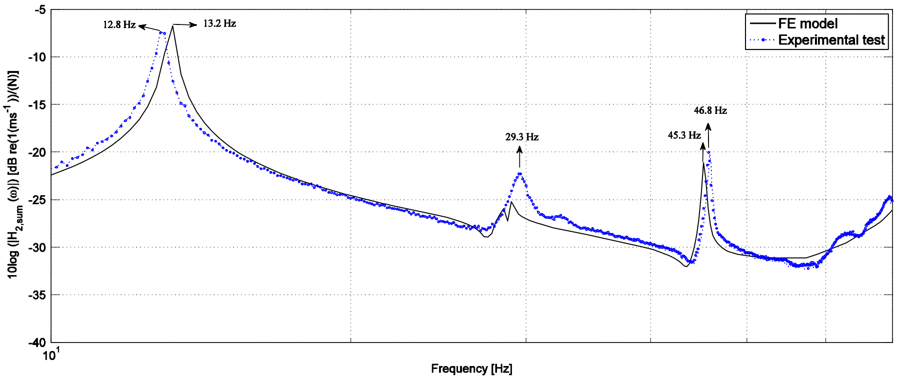

(b) RP2 (j = 2)

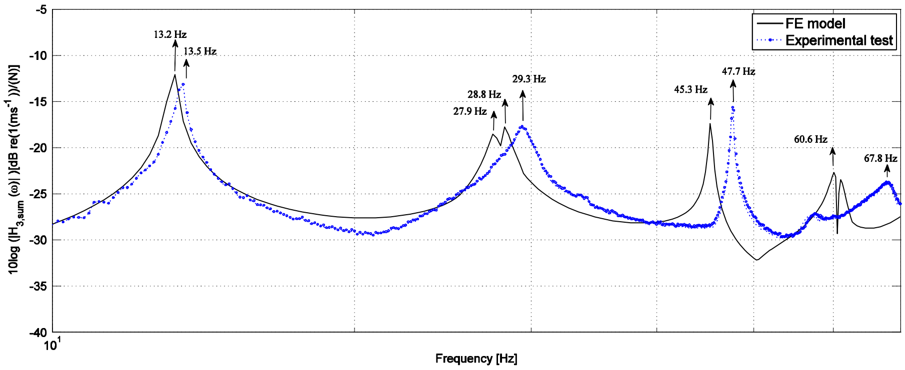

(c) RP3 (j = 3)

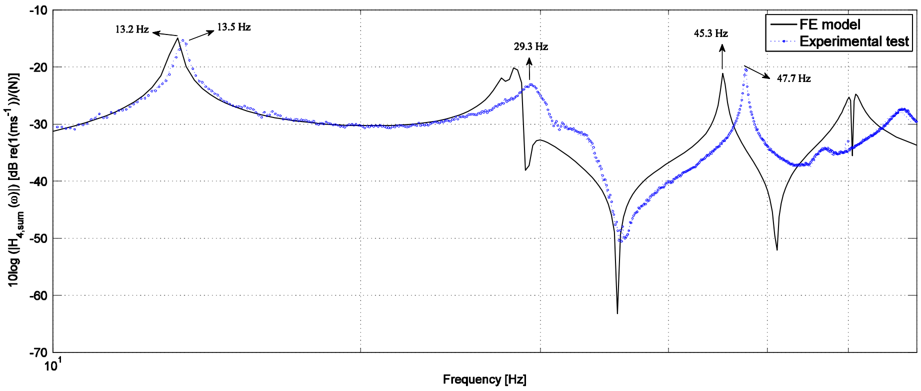

(d) RP4 (j = 4)

Fig. 5 Continued

3.2 Mobility of the floating-floor system

Fig. 6 shows mobility values (see Eq. (2)) measured at three distinct points. The results are shown for a narrow frequency band 10Hz -70Hz. It is seen that with the introduction of a steel block between the impulsive force and the steel plate, the values were reduced and consequently the vibration insulation improved. The use of this solid steel block caused a reduction of at least 5 dB over most of the frequency range.

Nevertheless, it is seen that the frequency responses were not sensitive to the floating condition, i.e., to the viscoelastic properties of the resilient material (recycled rubber). The velocity transfer function, as defined in Eq. (2) depends strongly in the size and nature of the structure. It is shown in Fig. 6 that the vibration reduction due to the inclusion of a block mass affects the nature of the excitation, which becomes a velocity source. In other words, the addition of a compact mass resulted in the increase of the driving point impedance, whereas the increase of damping (e.g., adding the rubber pad) did not affect the driving point impedance.

For the blue continuous line, no isolator were fitted, i.e., the receiver (steel plate) connected directly to the source (compact mass), then the mobility of the isolator should be assumed to be null (rigid link). Comparing the blue continuous line and the dashed black line, it is evident that the isolator effectiveness, which is defined by the ratio of the receiver velocity with no isolator to that with isolator fitted, is very low. For practical problems, the isolator effectiveness should be as high as possible for good isolation.

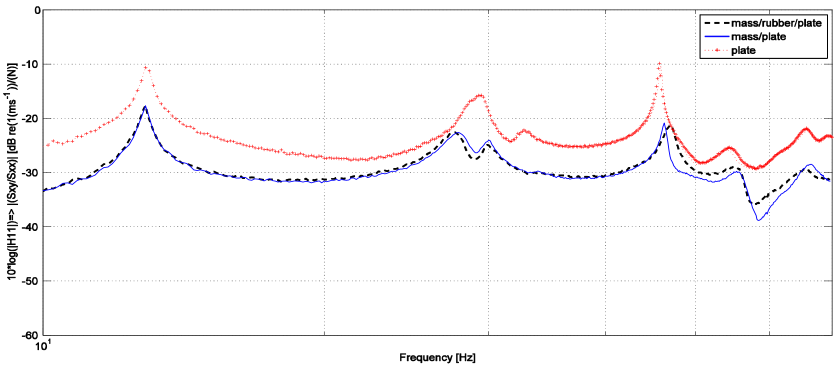

(a) Impulse force applied at F_1 (x = 540 mm; z = 665 mm)

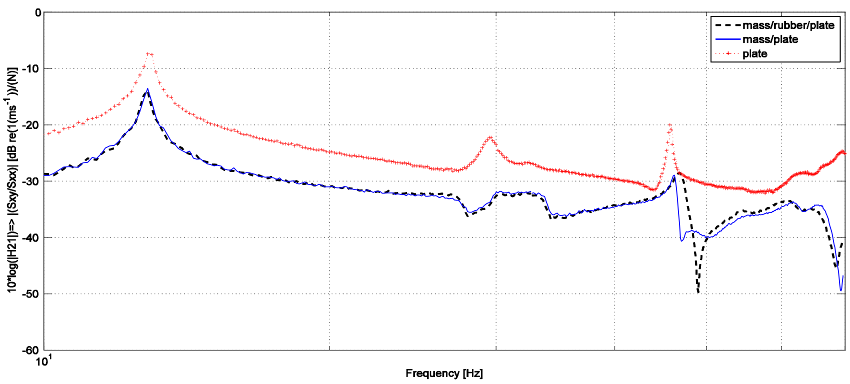

(b) Impulse force applied at F_2 (x = 555 mm; z = 325 mm)

Fig. 6 Experimental results for the amplitude of the FRF H_{11} (Eq. 2); The velocity responses were measured at RP_1(x = 550 mm; z = 0mm)

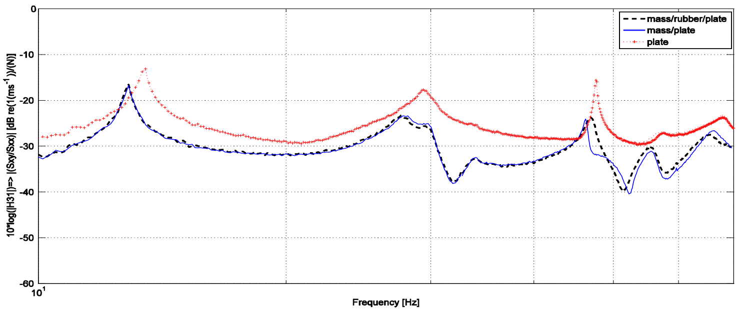

(c) Impulse force applied at F_3 (x = 285 mm; z = 300 mm)
Fig. 6 Continued

In Fig. 6 three FRFs were measured for the impulse excitation forces.

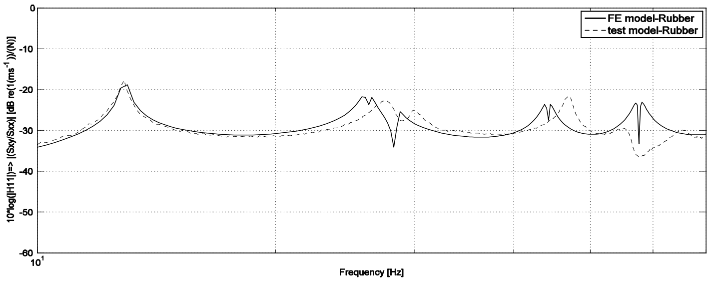

(a) FRF H_{11}

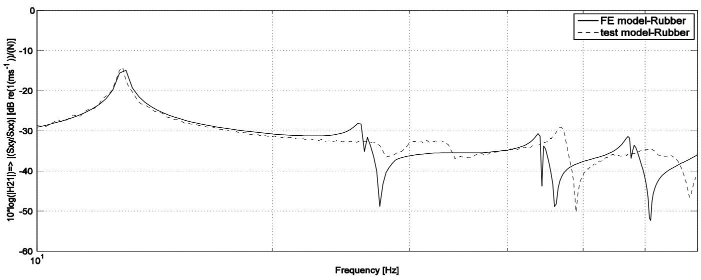

(b) FRF H_{21}

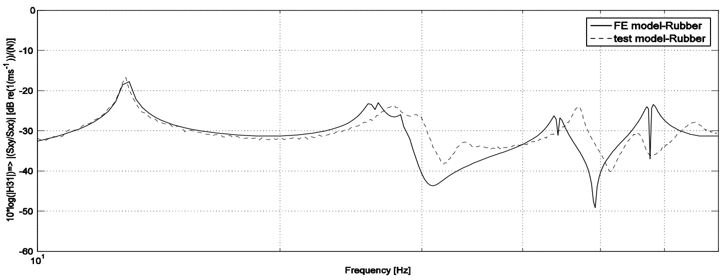

(c) FRF H_{31}

Fig. 7 Comparison between experimental and numerical (FE model) results for the amplitude of the FRFs (dB re 1 ms^{-1}/N) considering the floating steel compact mass

Fig. 7 presents a comparison between experimental and numerical (FE model) results for the amplitude of the FRFs considering the floating compact mass. A notable difference was observed between the measured and the estimated natural frequencies for the first five modes of vibration. However, bearing in mind that good correlation was obtained for the first three estimated and measured natural frequencies, it is believed that the modal data obtained are acceptable (see Table 2). The differences might be attributed to a lack of stiffness in the FE model.

Table 2 The natural frequencies below correspond to the first 5 modes of the coupled system steel plate/rubber/steel block

Vibration Mode Number	F_N [Hz] (FE model)	F_N [Hz] (Measured)	Correlation %
1	13.6	12.8	99.2
2	28.2	27.8	99.6
3	29.3	30.1	99.2
4	44.3	46.1	98.2
5	60.8	60.1	99.3

It is observed in Table 2, the relationship between measured and estimated coupled natural frequencies. There were significant correlations with values ranging from 98.2 to 99.6%.

3.3 The Influence of block mass and pad stiffness on the steel plate mean-square velocity

The results that are presented in Figures 8 and 9 were obtained via simulations using the modal model developed using Eqs. (4), (5) and (6) for a frequency range 10-200Hz. The analysis was based on considering the influence of some variations in the 'input' parameters, which are required in the pre-processing stage of a numerical experiment, and on the subsequent vibration transmission mechanisms of typical building configurations. Fig. 8 shows a parametric study of the influence of the compact mass on the vibration reduction and Fig. 9 the effects of the rubber pad stiffness on transmission.

It is seen in Fig. 8 that the effect of increasing the compact mass becomes more significant as frequency increases. At high frequencies the mean-square velocity increases with approximately +6dB/octave, i.e., like the impedance of an added mass.

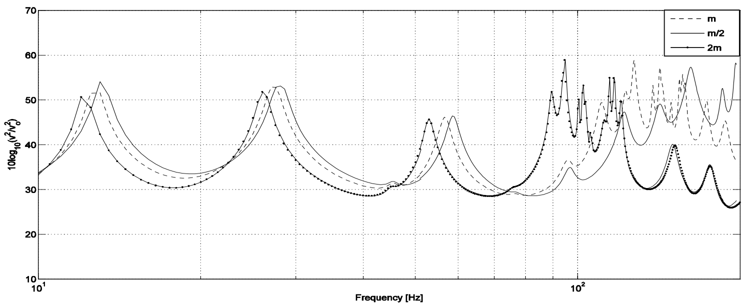

(a) Narrow frequency

Fig. 8 Variation of the mean-square velocity of the receiver (steel plate) with frequency for three different values of the steel block mass (m)

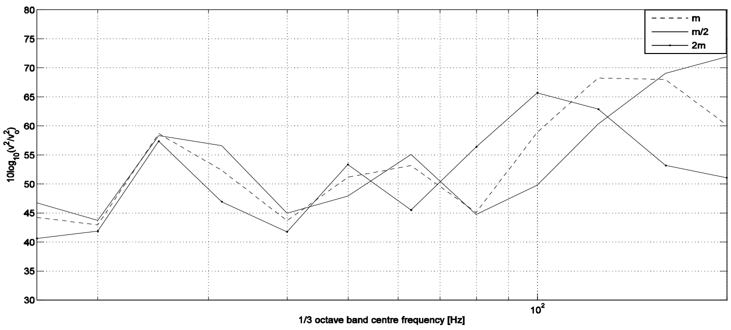

(b) one-third octave frequency centre

Fig. 8 Continued

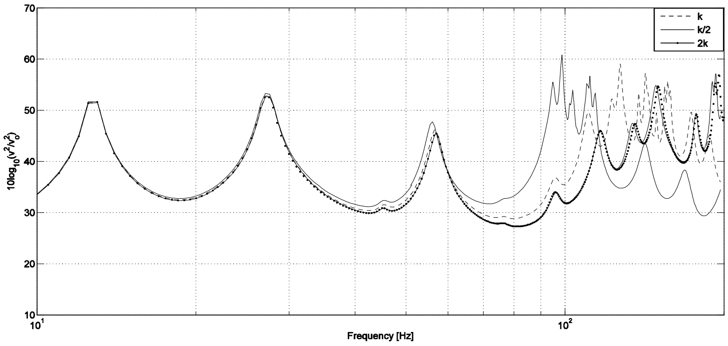

(a) Narrow frequency

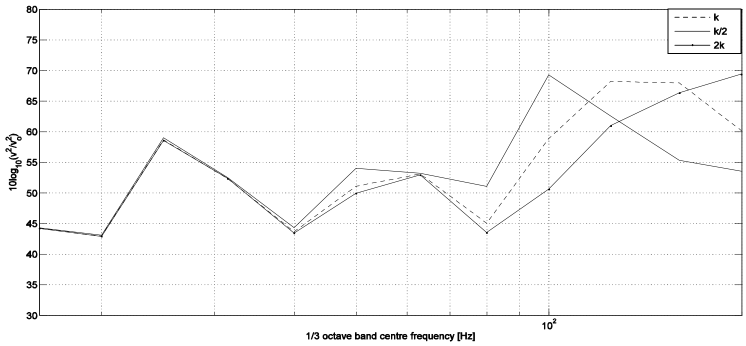

(b) one-third octave frequency centre

Fig. 9 Variation of the mean-square velocity of the receiver (steel plate) with frequency for three different values of the rubber pad stiffness (k)

Fig. 9 presents the variation of the mean-square velocity with frequency as the rubber pad stiffness varies. It is a popular measure to characterize the vibration isolation. In general, the basic idea for a good result is to design the structures on both side of the spring with much larger impedance than that of the spring.

The principle of reflecting structural waves occurs at the resilient element (rubber pad). It is well-known that a large velocity level attenuation across springs is a necessary requirement for effective vibration isolation. It is seen that as the stiffness of the spring increases in comparison to that of the steel plate, the steel plate velocity increases. As a result, the velocity level difference across the spring decreases and also the vibration isolation. In practical terms, after these results, the serviceability limit should be specified in accordance to the service and conditions, and the structural performance requirements.

4. Conclusions

According to the results obtained, it is seen that the effectiveness of the isolator depends not only on the source (impulsive force on the compact mass) mobility but also on the isolator (rubber pad) and receiver (steel plate) mobilities. It is required that the mobility of the isolator be much greater than that of the source and receiver. The mobility (and/or velocity) of the source (steel block) plus that of the steel plate can be very large (e.g., at resonance frequencies of the source and of the receiver. In general at low frequencies the transmitted force is controlled by the stiffness. It became clear the simple example presented here of a mass-spring system upon a flexible foundation is of limited practical value for vibration purposes. In practice, it is believed that the vibration isolation will be often much smaller than for this idealized case. Reasons are the non-rigidity of the source (compact mass) and isolator stiffening due to internal standing waves.

Moreover, vibration transmission may occur simultaneously for various vibration directions and also ‘flanking’ transmission may occur via airborne sound radiation. Due to these complexities, the mobilities as defined in this paper are of limited value for quantitative design applications. On the other hand, it gives a good qualitative insight with respect to system properties. An experimental analysis procedure which can handle multi-directional vibration will be treated in a future work.

The effects of vibration are becoming an increasingly important issue in the design of buildings and buildings elements. Modern construction methods mean that buildings are becoming lighter and have less structural damping. The response of such buildings to vibrations is therefore increased.

Thus, subjects using the buildings are more likely to experience vibration. In this situation, the velocity (and/or acceleration) vibration levels need to be assessed for all of the above approaches to ensure that the requirements of a particular code of practice (or standard) are met completely. The dynamic response of steel floors is an important issue in building structures and further work is required to consider a real structural floor, with the ultimate aim of comparing the real and the scaled prototype steel floor.

Acknowledgments

Thanks to FAPEMIG (The Research Foundation of Minas Gerais State), the official sponsor, and to UFMG (The Federal University of Minas Gerais, Brazil).

References

Abaqus/CAE (2005), “User’s Manual v6.7”.

Brownjohn, J.M.W. and Xia, P. (2000), "Dynamic assessment of curved cable-stayed bridge by model updating", *ASCE J. Struct. Eng*., **126**(2), 252-260.

Cremer, L., Heckl, M. and Petersson, B.A.T. (2005), *Structure Borne Sound*, Springer-Verlag Berlin.

Fahy, F.J. (1985), *Sound and Structural Vibration*, Academic Press London.

Fulford, R.A. and Gibbs, B.M. (1997), "Structure-borne sound power and source characterization in multi-point-connected systems, part 1: case studied for assumed force distributions", *J. Sound Vib.*, **204**(4), 659-77.

Fulford, R.A. and Gibbs, B.M. (1999), "Structure-borne sound power and source characterization in multi-point-connected systems, part 2: about mobility functions and free velocities", *J. Sound Vib.,* **225**(2), 239-282.

Langley, R.S. (2007), "Numerical evaluation of the acoustic radiation from planar structures with feneral baffle conditions using wavelets"*, J. Acoust. Soc. Am*., **121**, 766-777.

Leppington, F.G., Broadbent, E.G. and Heron, K.H. (1982), "The acoustic radiation efficiency of rectangular panel", *CMES: Proceedings of the Royal Society of London, Series A, Math Physical Sciences*, **382**, 245-271.

Mak, C.M. and Su, J.X. (2002), "A power transmissibility method for assessing the performance of vibration isolation of building services equipment", *Appl. Acoust.*, **63**(12), 1281-1299.

Mondot, J.M. and Petersson, B.A.T. (1987), "Characterization of structure-borne sound sources: the source descriptor and coupling function", *J. Sound Vib.*, **114**, 507-18.

Pan, J., Guo, J. and Ayres, C. (2005), "Improvement of sound absorption of honey-comb panels", *Proceedings of Acoustics*, Busselton, Western Australia.

Pavic, A. and Reynolds, P. (2003), "Modal testing and dynamic FE model correlation and updating of a prototype high-strength concrete floor", *Cement and Concrete Composites*, **25**, 787-799.

Petersson, B.A.T. and Gibbs, B.M. (2000), "Towards a structure-borne sound source characterization", *Appl. Acoust.* **63**(12), 325-343.

Rao, S.S. (1995), *Mechanical vibrations*, Third Edition, Addison-Wesley.

Remillieux, M.C. (2012), "External pressure loading, vibration, and acoustic responses at low frequencies of building components exposed to impulsive sound", *Applied Acoustics***, 73**, 1059-1075.

Sanz, R.M., Castizo, M.M. and Gomez, R.V. (2011), "The performance of resilient layers made from recycled rubber fluff for impact noise reduction", *Applied Acoustics*, **72**, 823-828.

Vigoureux, D. and Guyader, J.L. (2012), "A simplified time reversal method used to localize vibrations sources in a complex structure", *Applied Acoustics*, **73**, 491-496.